Wind-Driven Angular Dependence of Sea-Surface Reflectance Measured with an Airborne Doppler Lidar

David M. Tratt and Robert T. Menzies
Jet Propulsion Laboratory, California Institute of Technology
4800 Oak Grove Drive, Pasadena, CA 91109, USA
Phone: (818)354-2750, Fax: (818)393-6984, Email: David.M.Tratt@jpl.nasa.gov

Dean R. Cutten
University of Alabama in Huntsville, Global Hydrology and Climate Center
977 Explorer Boulevard, Huntsville, AL 35806, USA

1 Introduction

The effects of wind-stress on the optical properties of the ocean surface have been studied for several decades. In particular, the classic study by Cox and Munk (1954) linking sea-surface wind field to wave slope statistics provides a phenomenology by which the sea-surface wind velocity can be estimated from direct measurement of the wave-modulated surface reflectance. A limited number of studies along these lines have been conducted using airborne (Bufton *et al.*, 1983; Hoge *et al.*, 1984) or spaceborne (Menzies and Tratt, 1996) lidar systems. In these instances, truthing was provided by *in situ* ship reports or satellite microwave remote sensing instruments (e.g., ERS scatterometer, SSM/I).

During the second deployment of the MACAWS (Rothermel *et al.*, 1998a,b) Doppler wind lidar in the summer of 1996 measurements of sea-surface reflectance as a function of azimuth- and nadir-viewing angles were acquired off the California coast. MACAWS data products include directly measured winds, as well as calibrated backscatter/reflectance profiles, thus enabling comparison of the winds inferred from sea-surface reflectance measurements with those deriving from the Doppler-processed direct line-of-sight (LOS) estimates. Additional validation data was extracted from the ERS and SSM/I satellite microwave sensor archives maintained by the JPL Physical Oceanography Distributed Active Archive Center (PO-DAAC).

2 Instrument description

MACAWS is a scanning coherent detection Doppler lidar based on CO_2 laser technology. Its salient operational characteristics are given in Table 1. Further details concerning instrumental parameters and performance can be found in Rothermel *et al.* (1998a,b).

MACAWS is a side-viewing instrument with the capability of being scanned in any direction within a ~64° full cone angle by means of a dual rotary germanium wedge scanner (Amirault and DiMarzio, 1985).

PARAMETER	VALUE
Wavelength	10.6 μm
Pulse energy	0.8 J
Pulse duration	3 μs
Pulse repetition frequency	20 Hz
Beam divergence	~0.3 mrad
Line-of-sight range resolution	300 m
Line-of-sight velocity resolution	~1 m/s

Table 1. MACAWS primary instrumental operating characteristics.

3 Experiment description

The experiment was conducted from the NASA DC-8 research aircraft on June 10, 1996 during the interval 17:00 - 17:30 UTC off the California coast at 124.°0W longitude, 38.°5N latitude. A flight altitude of 20000ft (6 km) was selected in order to provide for high signal-to-noise ratio for the ocean surface return whilst precluding the likelihood of saturating the detection system. At this altitude the lidar footprint area at the ocean surface is ~3/sinθ m^2, θ being the nadir viewing angle.

Because the maximum beam depression angle available with the present scanner is only 30°, access to nadir viewing angles less than 60° necessitated controlled banking of the aircraft. With the scanner staring abeam of the aircraft and set for maximum depression, the DC-8 was thus flown in a series of nested circular tracks with progressively steeper bank angles in order to access a

series of nadir angle viewing geometries down to θ = 20°. Each circular flight track segment in this manner essentially represents a VAD (velocity-azimuth display) acquisition configuration. The lidar was operated at 20-Hz pulse repetition frequency and data were logged in the form of 3-pulse averages.

4 Theory of ocean surface optical scattering

Due to the absorptive properties of water at the MACAWS operating wavelength, any contribution to the total reflectance due to subsurface scatter can be neglected, so that the retroreflectance, R, of the wind-stressed sea surface may be expressed by:

$$R = \frac{\rho(1-F)\sec^4\theta}{2\pi\langle s^2\rangle} \exp\left[-\frac{\tan^2\theta}{\langle s^2\rangle}\right] + \frac{FR_F\cos\theta}{\pi} ,$$

where ρ is the Fresnel reflectance of seawater for normal incidence (computed assuming the Pacific Ocean refractive index data of Querry *et al.* [1977]) and $\langle s^2\rangle$ is the wind-driven capillary wave mean-square slope estimated according to Cox and Munk (1954). R_F is the reflectance of sea foam (proportional coverage F). Comparatively little information is available in relation to the value of R_F in the thermal infrared spectral region. Salisbury *et al.* (1993) conducted a series of measurements which concluded that the 8-14 μm foam reflectance was similar in magnitude to that of the seawater itself (i.e., $R_F = \rho$); an assumption which we will follow here.

Assuming the wind-dependent foam coverage parameterization deduced by Koepke (1984), the modeled dependence of the ocean backscatter on wind speed (U_{10} - the wind speed at 10-m altitude above the water surface) and nadir viewing angle, as computed using the above expression, is depicted in Figure 1. From this display we observe that scattering at low angles derives primarily from the specular component reflected from capillary wave facets, while at the larger nadir angles the Lambertian-distributed contribution from foam dominates.

5 Field measurements

As described in Section 3 above, a series of circular tracks were flown above an unobscured (clear sky) ocean target at different lidar incidence angles. The resultant time series data were inverted to obtain range-resolved profiles of absolute backscatter and the sea-

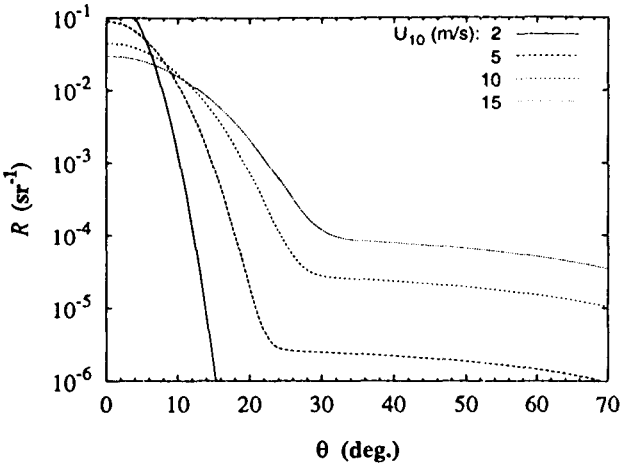

Figure 1. Modeled 10.6-μm sea-surface reflectance as a function of nadir angle and wind speed. The abrupt change in gradient marks the distinction between foam- and capillary wave-dominated reflectivity regimes.

surface returns were integrated with respect to range in order to extract the azimuthal dependence of the surface reflectance. One such azimuthal scan is represented in Figure 2. Acquired at a nadir viewing angle of 50°, this dataset has been processed by an 8x smoothing function to eliminate speckle-induced outliers arising from the combination of glint returns from the ocean surface with the three-fold pulse averaging of the raw data.

The near-surface horizontal wind estimated from the LOS Doppler retrievals is variable 5-8 m/s with the crosswind vector at ~150° approximate azimuth. Inspection of Fig. 1 indicates that we may expect foam reflectance to dominate in this data example, and indeed the retrieved surface reflectance appears to corroborate this assertion. Furthermore, the azimuthally-resolved data presented in Fig. 2 evince an asymmetric polar signature, implying that the differential nature of $\langle s^2\rangle$ in the upwind/downwind and crosswind axes expounded by Cox and Munk (1954) is transferred to the foam coverage also.

6 Conclusion

Measurements of the azimuthal and incidental angular dependence of sea-surface backscatter have been conducted with an airborne Doppler lidar operating at a wavelength of 10.6 μm in the mid-infrared. Line-of-sight

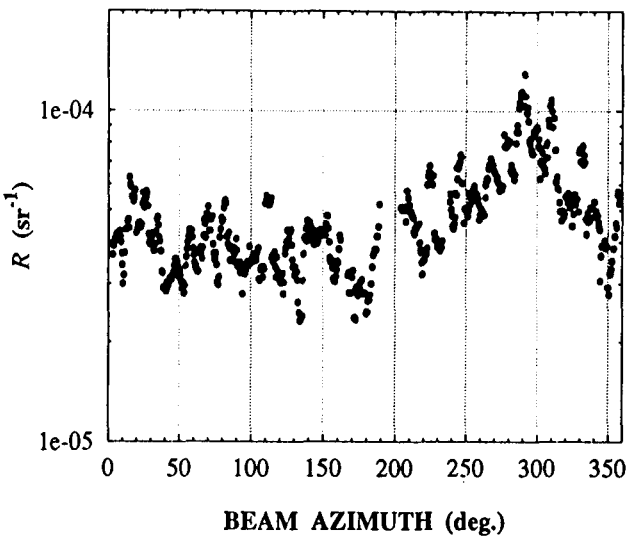

Figure 2. Azimuthal dependence of the sea-surface reflectance at a nadir viewing angle of 50°. The azimuth angle expresses the lidar view heading relative to due North.

wind velocity estimates also provided by the lidar data stream permit comparison of the directly measured wind field against those inferred from analysis of the surface reflectance data. This dataset will provide further insight into the mid-infrared optical effects of the air-sea interaction, thereby contributing to a fuller understanding of radiation transfer between the ocean and atmosphere.

Acknowledgment

This work was carried out by the Jet Propulsion Laboratory, California Institute of Technology, under contract with the National Aeronautics and Space Administration.

References

Amirault, C. T., and C. A. DiMarzio (1985). Precision pointing using a dual-wedge scanner. *Appl. Opt.*, **24**(9), 1302-1308.

Bufton, J. L., F. E. Hoge, and R. N. Swift (1983). Airborne measurements of laser backscatter from the ocean surface. *Appl. Opt.*, **22**(17), 2603-2618.

Cox, C., and W. Munk (1954). Measurement of the roughness of the sea surface from photographs of the Sun's glitter. *J. Opt. Soc. Amer.*, **44**(11), 838-850.

Hoge, F. E., W. B. Krabill, R. N. Swift (1984). The reflection of airborne UV laser pulses from the ocean. *Marine Geodesy*, **8**(1-4), 313-344.

Koepke, P. (1984). Effective reflectance of oceanic whitecaps. *Appl. Opt.*, **23**(11), 1816-1824.

Menzies, R. T., and D. M. Tratt (1996). Ocean surface wind speed determination with LITE surface directional reflectance measurements. *18th International Laser Radar Conference Abstracts* (Berlin, July 1996), p.76.

Querry, M. R., W. E. Holland, R. C. Waring, L. M. Earls, and M. D. Querry (1977). Relative reflectance and complex refractive index in the infrared for saline environmental waters. *J. Geophys. Res.*, **82**(9), 1425-1433.

Rothermel, J., D. R. Cutten, R. M. Hardesty, R. T. Menzies, J. N. Howell, S. C. Johnson, D. M. Tratt, L. D. Olivier, and R. M. Banta (1998a). The Multi-center Airborne Coherent Atmospheric Wind Sensor, MACAWS. *Bull. Amer. Meteorol. Soc.*, **79**, April 1998.

Rothermel, J., L. D. Olivier, R. M. Banta, R. M. Hardesty, J. N. Howell, D. R. Cutten, S. C. Johnson, R. T. Menzies, and D. M. Tratt (1998b). Remote sensing of multi-level wind fields with high-energy airborne scanning coherent Doppler lidar. (*http://epubs.osa.org/oearchive/pdf/4016.pdf*) *Opt. Express*, **2**(2), 40-50.

Salisbury, J. W., D. M. D'Aria, and F. F. Sabins, Jr. (1993). Thermal infrared remote sensing of crude oil slicks. *Remote Sens. Environ.*, **45**(2), 225-231.